Published in final edited form as:
Mol Cancer Ther. 2015 January ; 14(1): 120–128. doi:10.1158/1535-7163.MCT-14-0366.

Tumor-Penetrating iRGD Peptide Inhibits Metastasis

Kazuki N. Sugahara[1,2], **Gary B. Braun**[1,3], **Tatiana Hurtado de Mendoza**[1], **Venkata Ramana Kotamraju**[1], **Randall P. French**[4], **Andrew M. Lowy**[4], **Tambet Teesalu**[1,5], and **Erkki Ruoslahti**[1,3]

[1]Cancer Research Center, Sanford-Burnham Medical Research Institute, La Jolla, California, USA

[2]Department of Surgery, Columbia University College of Physicians and Surgeons, New York, New York, USA

[3]Center for Nanomedicine and Department of Cell, Molecular and Developmental Biology, University of California Santa Barbara, Santa Barbara, California, USA

[4]Division of Surgical Oncology and Moores Cancer Center, University of California, San Diego, La Jolla, California, USA

[5]Centre of Excellence for Translational Medicine, University of Tartu, Tartu, Estonia

Abstract

Tumor-specific tissue-penetrating peptides deliver drugs into extravascular tumor tissue by increasing tumor vascular permeability through interaction with neuropilin (NRP). Here we report that a prototypic tumor-penetrating peptide iRGD (amino acid sequence: CRGDKGPDC) potently inhibits spontaneous metastasis in mice. The anti-metastatic effect was mediated by the NRP-binding RXXK peptide motif (CendR motif), and not by the integrin-binding RGD motif. iRGD inhibited migration of tumor cells and caused chemorepulsion *in vitro* in a CendR- and NRP-1-dependent manner. The peptide induced dramatic collapse of cellular processes and partial cell detachment, resulting in the repellent activity. These effects were prominently displayed when the cells were seeded on fibronectin, suggesting a role of CendR in functional regulation of integrins. The anti-metastatic activity of iRGD may provide a significant additional benefit when this peptide is used for drug delivery to tumors.

Keywords

tumor-penetrating peptides; C-end Rule; neuropilin; metastasis; chemorepulsion

Corresponding Author: Kazuki N. Sugahara, Sanford-Burnham Medical Research Institute, 10901 North Torrey Pines Road, La Jolla, CA 92037., Phone: 858-646-3100 x3517; Fax: 858-795-5353; sugahara@sanfordburnham.org.

Conflict of Interest: K.N. Sugahara, V.R. Kotamraju, T. Teesalu, and E. Ruoslahti have ownership interest (including patents) in CendR Therapeutics Inc. E. Ruoslahti is also founder, chairman of the board, consultant/advisory board member of CendR Therapeutics Inc. No potential conflicts of interest were disclosed by the other authors.

Introduction

Tumor blood vessels are structurally defective (1). They often lack pericytes, and their basement membrane is abnormally loose. The irregular structure leads to leakiness and predisposes tumors to metastasis. The leakiness of tumor vasculature also results in high interstitial fluid pressure, which prevents drug penetration into tumor tissue (2). Poor drug penetration reduces the potential for anti-tumor efficacy and results in acquired drug resistance. Factors that increase vascular permeability, such as vascular endothelial growth factor (VEGF), bradykinin, and nitric oxide, improve drug distribution into tumor tissue, but can also promote metastasis by enhancing tumor cell access to and from blood vessels (2–4). miR-105, a micro RNA that disrupts vascular integrity and increases vascular permeability facilitates metastasis formation (5). Forced expression of miR-105 in non-metatatic tumor cells leads to enhanced vascular permeability and metastasis, while inhibition of miR-105 in highly metastatic tumor cells suppresses metastasis.

Neuropilin-1 (NRP-1) and neuropilin-2 (NRP-2) are some of the key molecules that regulate vascular permeability (6). Tissue-penetrating peptides bind to NRPs through the consensus RXXR/K amino acid sequence, increasing vascular permeability and transport of molecules through tissue (7). The RXXR/K sequence motif is not active unless it occupies a C-terminal position in a peptide, therefore referred to as the C-end Rule (CendR) motif (8). Notably, many natural ligands for NRPs, such as VEGF and class 3 semaphorins, carry a CendR motif, and share various biological activites with tissue-penetrating peptides (6, 7).

iRGD (cyclic CRGDK/RGPD/EC; the CRGDKGPDC form was used in this study) is a prototypic tumor-specific tissue-penetrating peptide, which delivers drugs deep into extravascular tumor tissue (9). Intravenously injected iRGD first targets αv integrins specifically expressed on tumor vasculature (10). iRGD is then proteolytically processed into CRGDK/R, exposing an active CendR motif at the C-terminus. The interaction of the CendR motif with NRPs initiates an active bulk transport system through the tumor tissue, allowing drugs conjugated to iRGD, and even free drugs co-administered with iRGD, to extravasate and spread within the tumor tissue (11). Thus, iRGD provides a simple way to enhance the theraputic index of various anti-cancer drugs. However, the effect of iRGD on the permeability of tumor blood vessels has led to a hypothetical concern that iRGD may promote metastasis through antidromic tumor cell dissemination into the circulation (12). While our earlier studies have shown that iRGD does not promote seeding of non-metastatic tumor cells (11), the effects of iRGD on metastatic tumors remain elusive. Here, we have examined the iRGD effects on spontaneous metastasis formation in mice bearing aggressive cancers.

Methods

Peptides, cells, tumor models, and in vivo treatment studies

Peptides were synthesized as described (8, 9, 11). PC-3 human prostate cancer cells were purchased from and authenticated by American Type Culture Collection. GFP-PC-3 cells were prepared by infecting the PC-3 cells with GFP lentiviruses (9, 13). LM-PmC cells were prepared by stable mCherry transduction in LM-P cells, which were derived from liver

metastasis of pancreatic ductal adenocarcinoma (PDAC) in *Kras$^{G12D/+}$;LSL-Trp53$^{R172H/+}$;Pdx-1-Cre* (KPC) mice and authenticated as described earlier (14). Both cell lines were cultured in Dulbecco's Modified Eagle Medium (DMEM) supplemented with 10% fetal bovine serum (FBS) and penicillin/streptomycin, and used for no longer than 6 months before being replaced. Tumor mouse models were created by orthotopic injections of 1 million GFP-PC-3 or LM-PmC cells into nude mice 2 weeks (GFP-PC-3) or 1 week (LM-PmC) prior to the initiation of the treatment study. The mice were intravenously treated every other day with 4 μmol/kg of peptides or vehicle (PBS) alone. After 21 days (GFP-PC-3) or 14 days (LM-PmC) of treatment, the mice were dissected under deep anesthesia, imaged under UV light with an Illumatool Bright Light System LT-9900 (Lightools Research, Encinitas, CA), and perfused through the heart with PBS containing 1% bovine serum albumin (BSA) prior to harvesting tissues. All animal experimentation was performed according to procedures approved by the Animal Research Committee at Sanford-Burnham Medical Research Institute, La Jolla, CA.

Flow cytometry

The experiments were performed as described previously (9). The primary antibodies were rabbit anti-human NRP-1 b1b2 prepared in-house as by immunizing rabbits with a human NRP-1 b1b2 protein, goat anti-human NRP-2 (R&D Systems, Minneapolis, MN), mouse anti-human αvβ3 (LM609) (EMD Millipore, Billerica, MA), mouse anti-human αvβ5 (P1F6) (EMD Millipore), rat anti-mouse αv (RMV-7) (eBioscience, San Diego, CA), rat anti-mouse α5 (MHR5) (SouthernBiotech, Birmingham, AL), mouse anti-human α5β1 (JBS5) (Thermo Scientific, Waltham, MA), mouse anti-human β1 (TS2/16) (eBioscience), mouse anti-human active β1 (HUTS-4) (EMD Millipore), rat anti-mouse β1 (HMb1-1) (eBioscience), and rat anti-mouse active β1 (9EG7) (BD Biosciences). The primary antibodies were detected with corresponding secondary antibodies conjugated to Alexa 488, 594 or 647 (Molecular Probes, Eugene, OR). The cells were analyzed with an LSR Fortessa System (BD Biosciences, San Jose, CA), and the data were analyzed with a Flowjo software.

In vitro peptide internalization assay

As described elsewhere (8, 9), tumor cells were grown on collagen type-I-coated coverslips (BD Biosciences) overnight in fully supplemented DMEM, incubated with 10 μM of fluorescein-conjugated iRGD (FAM-iRGD) or FAM-labeled iNGR peptide (cyclic CRNGRGPDC) in the presence of 10 μg/ml of anti-NRP-1 b1b2 or control IgG for 4 hours. The cells were washed with warm PBS, fixed in 4% paraformaldehyde (PFA), stained with DAPI (Molecular Probes), and observed under a Fluoview 500 confocal microscope (Olympus America, Center Valley, PA).

In vivo peptide homing assay

As described previously (9), 100 μg of peptide in PBS were intravenously injected into tumor mice, and allowed to circulate for 60 minutes. The mice were perfused through the heart with PBS containing 1% BSA, and tissues were harvested and processed for

immunofluorescence. The tissue sections were examined by a Fluoview 500 confocal microscope.

Transwell migration assay

Cell migration was analyzed using 24-well Transwell chambers containing polycarbonate membranes with 8-μm pores (Corning Inc., Corning, NY) (15). Both sides of the membranes were coated with 50 μg/ml of collagen type-I (BD Biosciences) to facilitate initial cell attachment to the membranes. GFP-PC-3 (4×10^4 cells) or LM-PmC (2×10^5 cells) cells in DMEM containing 0.1% BSA were added to the upper compartment. The lower compartment was filled with 600 μl of DMEM containing 0.1% BSA. Peptides at a final concentration of 10 μM or PBS were added to both the upper and lower compartments, or in some cases, only to the lower compartment. In some experiments, the cells were treated with 10 μg/ml of anti-NRP-1 b1b2 or control IgG (Abcam, Cambridge, MA) for 30 minutes prior to seeding and throughout the assay. After incubation in a CO_2 incubator at 37°C for 24 hours, the cells on the upper side of the membranes were gently wiped off, and the membranes were fixed in methanol and stained with hematoxylin and eosin. The membranes were mounted on glass slides, and imaged under a light microscope. The total number of cells that migrated to the lower side of the membranes was determined by counting cell numbers under low magnification (×100).

Chemorepulsion assay

Silver nanoparticles (AgNPs; diameter, 70 nm) were prepared as described (16). In brief, AgNPs synthesized by polyvinylpyrolidone/ethylene-glycol reduction method were precipitated with acetone, and redissolved in water. The AgNPs were then coated with NeutrAvidin (NA)-5 kDa polyethylene glycol (PEG)-Orthopyridyl disulfide (OPSS) (NA, Thermo Scientific; N-Hydroxysuccinimide-PEG-OPSS, JenKem Technology USA, Allen, TX), backfilled with lipoic-3 kDa PEG-amine (Nanocs, New York, NY), and labeled with amine-reactive CF555-succinimidyl ester dye (Biotium Inc., Hayward, CA). The NA-AgNPs were then coated with biotinylated peptides or with free biotin (Sigma-Aldrich, St. Louis, MO). iRGD-AgNPs, CRGDC-AgNPs, and AgNPs without any peptides were blotted along the periphery of glass-bottom wells by applying 10 μl drops of nanoparticle solutions on the glass surface and drying the drops in a laminar airflow chamber for 5 minutes. The wells were briefly rinsed with PBS three times, and 2×10^5 LM-PmC cells in full culture DMEM were seeded using a cloning cylinder in the center of the wells in close priximity with the AgNPs, or in some experiments, on top of the AgNP-covered areas. The cells were allowed to attach to the glass surface in a CO_2 incubator for 3 hours before the cylinder was removed, and further cultured in DMEM with 1% BSA for 24 hours. The wells were then subjected to live cell imaging by taking time-lapse images every 15 minutes for 48 hours with an Inverted IX81 Wide Field and Fluorescence Microscope equipped with CO_2 and Temperature Controlled Time Lapse System (Olympus America).

Cell attachment assay

The assays were performed following a protocol described elsewhere (17). Cells resuspended in DMEM containing 1% BSA were treated with peptides for 30 minutes at 37°C under mild rotation. The cells were seeded in 96-well plates coated with human

fibronectin (R&D Systems) or bovine collagen type-I (BioPioneer, San Diego, CA) at 4 × 10^5 cells/ml (LM-PmC) or 2 × 10^5 cells/ml (GFP-PC-3), and allowed to attach to the wells for 30 minutes at 37°C in a CO_2 incubator in the presence of the peptides. In some cases, the cells were treated with the peptides in the presence of 10 μg/ml of anti-NRP-1 b1b2 or control IgG, or treated solely with anti-human β1 (EMD Millipore) or anti-mouse β1 (eBioscience) integrin subunit antibodies or control IgG (Abcam). After the incubation, the cells were treated with 0.25% crystalline trypsin for 2 minutes, and the reaction was stopped by adding 0.5 mg/ml soybean inhibitor. The wells were gently washed with warm DMEM to remove detached cells, and the cells that remained attached to the wells were cultured in full DMEM containing 0.5 mg/ml of 3-(4,5-dimethylthiazol-2-yl)-2,5-diphenyltetrazolium bromide (MTT). Two hours later, the cells were lysed with a buffer containing dimethylsulfoxide and methanol at 1:1 volume ratio, and absorbance at 595 nm was read with a microplate reader.

In vitro cell retraction assay

Cells were cultured on fibronectin-coated coverslips for 1 hour at 37°C in a CO_2 incubator, and peptides were added at a final concentration of 10 μM. The cells were cultured for another 30 minutes at 37°C in a CO_2 incubator, fixed in 4% PFA, stained with a rabbit anti-phospho-paxillin pTyr118 antibody (Pierce Biotechnology, Rockford, IL) and DAPI, and imaged under a Fluoview 500 confocal microscope. The anti-phospho-paxillin pTyr118 was detected with an Alexa488 donkey anti-rabbit antibody (Molecular Probes).

Statistical analysis

Data were analyzed by two-tailed Student's t-test, one-way analysis of variance (ANOVA) followed by suitable post-hoc test, or Pearson's test. The results are summarized in Supplementary Table S1.

Results

iRGD inhibits prostate cancer metastasis in a CendR-motif dependent manner

We tested the effect of the iRGD peptide (cyclic CRGDKGPDC) on metastasis by giving intravenous injections of iRGD to mice bearing orthotopic xenograft tumors of GFP-labeled PC-3 human prostate cancer cells (GFP-PC-3), which develop spontaneous metastases in various organs (13). GFP-PC-3 cells express high levels of cell surface αv integrins and NRPs (Fig. 1A). *In vivo*, the blood vessels and tumor cells in orthotopic and metastatic GFP-PC-3 tumors are effective targets for iRGD (9, 11). Intravenous iRGD injections repeated every other day over three weeks significantly inhibited spontaneous metastasis (Fig. 1B and C). The anti-metastatic effect of iRGD was dependent on the NRP-binding RXXK CendR motif because RGDfV, a conventional cyclic RGD peptide that lacks a CendR motif (10, 11), and iRGDD (CRGDDGPKC), a scrambled iRGD with a disrupted CendR motif (11), did not inhibit metastasis. iRGD slightly inhibited primary tumor growth (Fig. 1D). However, no significant correlation was found between the weight of the primary tumor and metastatic burden (Supplementary Fig. S1A) indicating that delayed growth of the primary tumor was not a significant cause of the iRGD-mediated metastasis inhibition. The finding

that iRGD treatment alone has minor effect on primary tumor growth is consistent with previous reports (9, 11).

iRGD and another tumor-penetrating CendR peptide, iNGR, inhibit pancreatic cancer metastasis

We also tested iRGD in a transplantable PDAC mouse model. The model was created by orthotopic inoculation of mCherry-labeled LM-P (LM-PmC) cells. The LM-PmC cells were established from a liver metastasis of *de novo* PDAC in KPC mice, which carry *K-Ras* and *p53* mutations that are commonly found in human PDACs (14, 18). The cells express αv integrins and NRPs, and are effectively targeted by iRGD *in vitro* and *in vivo* (Supplementary Fig. S2). iRGD also inhibited metastasis in this model (Fig. 2A and B), whereas iRGDD, and another non-CendR cyclic RGD peptide, CRGDC (19), did not, indicating dependence of the activity on the CendR motif in iRGD. We also tested another tumor-specific CendR peptide, iNGR (CRNGRGPDC), which targets a variant CD13 in tumor vessels with its NGR motif, and accomplishes NRP-dependent tumor penetration with its CendR motif (20). iNGR effectively internalized into LM-PmC cells *in vitro* and targeted LM-PmC tumors *in vivo* (Supplementary Fig. S2B and C). Prolonged systemic treatment with this peptide also inhibited metastasis in the LM-PmC model, further supporting the role of the CendR motif in the activity. Neither iRGD nor iNGR affected primary tumor growth in this model (Fig. 2C).

Conventional RGD peptides block tumor cell seeding to tissues by interfering with αv integrin functions, inhibiting experimental metastasis created from intravenously injected tumor cells (10). However, these monomeric peptides have little effect on spontaneous metastasis, which involves the entire metastatic cascade (21). Even RGD-coated nanoparticles, which bind to integrins with higher avidity and have a longer half-life than the free peptide, have limited effect on spontaneous metastasis unless the particles are loaded with anti-neoplastic drugs (22). Our results are in line with these earlier findings. CRGDC has a similar affinity to αv integrins as iRGD (9), and inhibits tumor cell attachment to vitronectin as effectively as iRGD (Supplementary Fig. S3). RGDfV has a nearly 10-fold higher affinity to αv integrins than CRGDC (23), and is an even more potent inhibitor of tumor cell attachment to vitronectin than iRGD and CRGDC. Neither CRGDC nor RGDfV inhibited spontaneous metastasis at the dose used for the CendR peptides (refer to Figs. 1 and 2), indicating that the iRGD effects are not mediated by the inhibition of αv-dependent cell attachment.

iRGD inhibits tumor cell migration in vitro

We next studied the effect of iRGD and other CendR peptides on tumor cell motility in search for a possible mechanism of the anti-metastatic activity. iRGD and iNGR, as well as RPARPAR, a non-tumor specific NRP-binding CendR peptide (8), significantly inhibited random migration of LM-PmC and GFP-PC-3 cells in Transwell assays (Fig. 3A and B). An anti-NRP-1 b1b2 antibody, which blocks CendR peptide binding to the NRP-1 b1b2 domain (24), dose-dependently inhibited the effects of the peptides. CRGDC and RGDfV had no effect on cell migration at the dose used for the CendR peptides. None of the CendR peptides affected tumor cell proliferation *in vitro* (Supplementary Fig. S4).

iRGD has chemorepulsive properties

Tumor cell migration in the Transwell system was also inhibited when iRGD was added only to the lower chamber (the chamber into which the cells migrate), suggesting that iRGD has chemorepulsive properties (Fig. 3C). Accordingly, we developed a chemorepulsion assay based on synthetic AgNPs to further study tumor cell response to iRGD. iRGD-coated AgNPs (iRGD-AgNPs), CRGDC-coated AgNPs (CRGDC-AgNPs), and plain AgNPs were immobilized on a glass surface, and tumor cells were seeded in the center in close proximity to the AgNPs using a cloning cylinder (Supplementary Fig. S5). Live cell imaging showed that LM-PmC cells were repelled by iRGD-AgNPs (Fig. 4A and Supplementary Movie SM1). Imaging at single cell level showed dramatic collapse of cellular protrusions and inhibition of migration beyond the boundary line of iRGD-AgNPs (Supplementary Movies SM2 and SM3). Single cells that landed on surfaces coated with iRGD-AgNPs lost contact with the surface and died likely through anoikis (10), while cells that attached to non-coated surfaces spread and remained adherent. In contrast, the cells were attracted to CRGDC-AgNPs, in line with the capability of traditional RGD peptides to serve as a scaffold for cell attachment, spreading, and survival (10) (Supplementary Movie SM4). The cells randomly invaded areas coated with plain AgNPs (Supplementary Movie SM5). We next seeded cells onto surfaces coated densely with the AgNPs in order to force migration on the AgNPs. The cells migrated approximately 2-fold slower on iRGD-AgNPs than on plain AgNPs or CRGDC-AgNPs (Fig. 4B). These results show that iRGD has chemorepulsive properties, and confirm its inhibitory effects on cell migration.

iRGD inhibits tumor cell attachment to fibronectin through interaction with NRP-1

Semaphorin 3A (Sema3A), also known as collapsin, is a chemorepulsive glycoprotein that collapses and paralyzes neuronal growth cones to repel axons (25). Interestingly, Sema3A and other class-3 semaphorins have an internal CendR sequence (RNR/PR), which interacts with NRPs upon proteolytic activation by furin (26–28). Sema3A and semaphorin 3F (Sema3F) also repel non-neuronal cells. The apparent mechanism is weakening of cell attachment to fibronectin mediated by β1 integrins, leading to collapse of cellular processes, and inhibition of cell migration and metastasis, all in a NRP-dependent manner similar to the iRGD activities (28–31). The semaphorins also possess other iRGD-like properties such as enhancing vascular permeability and internalization into cells (3, 28, 29). A NRP-binding 22 amino acid peptide made from the C-terminus of Sema3A serves as a tumor-penetrating drug delivery carrier similar to iRGD (32). Thus, it appears that iRGD utilizes a similar mechanism as Sema3A in collapsing cellular processes and repelling tumor cells.

LM-PmC and GFP-PC-3 cells attach to fibronectin predominatly through a β1 integrin-mediated mechanism (Fig. 5A). The cells express high levels of surface β1 integrins, including α5β1, which primarily recognizes fibronectin (Fig. 5B) (10). A large proportion of their β1 integrins are in an active conformation. iRGD inhibited the tumor cell attachment to fibronectin in a dose-dependent manner (Figs. 6A and Supplementary Fig. S6A). Most conventional RGD peptides bind both to αv and α5β1 integrins (19, 23), whereas the RGD motif of iRGD is selective for αv integrin binding (9), suggesting that iRGD-induced cell retraction is not due to direct competition with fibronectin. Instead, the iRGD effects were reversed by anti-NRP-1 b1b2 antibodies, indicating a NRP-1-dependent mechanism (Figs.

6A and Supplementary Fig. S6A). CRGDC, which competes with fibronectin in α5β1 binding (19), inhibited tumor cell attachment to fibronectin in an RGD motif-dependent manner (Figs. 6B and Supplementary Fig. S6B). Anti-NRP-1 b1b2 had no effect on this activity. CRGDK, a post-cleavage mimic of iRGD, which binds to NRP-1 but has negligible RGD activity (9), inhibited cell attachment to fibronectin. iNGR and RPARPAR, CendR peptides without an RGD motif were also effective, but RPARPAR-NH_2, an RPARPAR variant with a blocked C-terminus that lacks affinity to NRPs (8), was not. Immunocytochemistry revealed that iRGD dramatically collapsed cellular protrusions on fibronectin-coated surfaces (Figs. 6C and Supplementary Fig. S6C). The cell retraction was accompanied by partial disassembly of focal adhesions, integrin-containing structures that mediate cell spreading and motility on fibronectin and other extracellular matrices (10, 33, 34). Two other CendR peptides, iNGR and RPARPAR, also caused collapse of cellular processes, whereas RPARPAR-NH_2 was inactive. These results suggest the possibility that iRGD inhibits tumor cell attachment to fibronectin by functional regulation of β1 integrins through interaction with NRP-1. Importantly, iRGD did not affect cell attachment to collagen type-I (Supplementary Fig. S7), which is mainly recognized by α1β1 and α2β1 integrins (35), suggesting that iRGD does not universally affect β1 integrins but selectively regulate fibronectin-binding integrins. Earlier studies have reported NRP-1-mediated endocytic removal of cell surface α5β1, which supports our observations (36).

Discussion

Here, we show that iRGD, the prototypic tumor-penetrating CendR peptide, is a potent inhibitor of metastasis, and provide evidence that a likely mechnism underlying the activity is inhibition of tumor cell migration and chemorepulsion mediated through binding of the CendR peptide motif to NRP-1. This study reveals a potentially important and useful anti-metastatic activity of iRGD, and removes the hypothetical concern (12) that iRGD might enhance metastasis.

Of the two active motifs in iRGD, the NRP-binding CendR motif is important for the anti-metastatic activity, whereas the integrin-binding RGD motif appears to be only needed to bring the peptide to the tumors or tumor cells. The evidence includes the lack of anti-metastatic activity by RGD peptides with no CendR motif, and the effective metastasis inhibition by iNGR, which uses a non-integrin receptor to home to tumors and is then processed to bind to NRP (20). Both NRP-1 and NRP-2 are highly expressed on tumor cells, and have been shown to play a role in metastasis (37). iRGD and iNGR bind to both NRP-1 and NRP-2 (20), suggesting the possibility that the metastasis inhibition is a combined effect through both NRPs.

Cell migration is a critical step in the metastatic cascade (38). It involves dynamic regulation of cellular protrusions, which mediate cell adhesion, provide traction to move, and sense environmental cues that attract or repel the cells (34, 39). Some cell migration inhibitors function as chemorepellents by collapsing frontal cellular protrusions to eliminate forward traction, which helps the cells to change direction (40). Various chemorepellents, including the natural CendR molecule Sema3A, inhibit metastasis by suppressing tumor invasion (28–30, 41). Our live cell imaging study showed that iRGD provided cues to retract cellular

protrusions, and conseqently repeled migrating tumor cell populations. The effect was dependent on the NRP-binding CendR motif because CRGDC, a non-CendR control peptide, was ineffective, and chemorepulsion by iRGD in Transwell assays was significantly inhibited by a blocking anti-NRP-1 b1b2 antibody. These findings demonstrate the CendR-dependent chemorepulsive properties of iRGD, and provide a potential mechanism to the anti-metastatic effects.

The retraction of cellular protrusions induced by iRGD appears to involve a NRP-1-mediated regulation of cell adhesion, which is prominently displayed on fibronectin-coated surfaces. The tumor cells we used in this study attach to fibronectin mainly through β1 integrins, suggesting that the de-adhesion of the protrusions induced by iRGD was through negative regulation of fibronectin-binding β1 integrins. Importantly, the effects of iRGD on the de-adhesion is clearly through CendR-NRP-1 interactions, as an anti-NRP-1 b1b2 antibody significantly blocked the iRGD effects, and other NRP-binding CendR peptides were effective while a CendR variant that lacks affinty to NRP was not. Thus, our results describe a string of CendR-mediated events, i.e., regulation of fibronectin-binding integrins, retraction of protrusions, and decreased avidity to fibronectin, which may contribute to the chemorepulsive properties of iRGD.

Our results question a general perception that NRPs are co-receptors that do not signal (37). NRPs lack a cytoplasmic signaling motif. Thus, it is thought that their central role is to modulate the functions of signaling receptors, such as VEGF receptor and plexin. However, the activities of the tumor-penetrating peptides we have used in this study suggest independent signaling by NRPs. The effects of our peptides resemble those of Sema3A with an important difference: Semaphorins are large proteins that have activities other than NRP binding, whereas the small size of our peptides and the fact that their only common denominator is the presence of a CendR motif, strongly suggest that NRP binding alone is responsible for the anti-metastatic and cell-repelling activities. Supporting this possibility, recent studies demonstrate that NRPs alone are capable of mediating various effects, such as endocytosis and phosphorylation of signaling adaptor molecules (6). Tumor-penetrating peptides may be ideal tools for dissecting intrinsic NRP functions.

The dose and administration schedules we used to establish the anti-metastatic effects of iRGD (and iNGR) were identical to those we have previously used to promote drug delivery into tumors (11). Thus, our results suggest that tumor-penetrating CendR peptides will simultaneously achieve metastasis inhibition when used as an adjuvant therapy to promote tumor-specific drug delivery. The anti-metastatic effects of iRGD could be useful in preventing initial metastasis, in suppressing additional metastasis when metastasis has already taken place, and in overcoming the prometastatic side effects of antiangiogenic therapies (41, 42).

Supplementary Material

Refer to Web version on PubMed Central for supplementary material.

Acknowledgments

Financial Support: This work was supported by grants R01CA167174 (K.N. Sugahara) and R01CA152327 (E. Ruoslahti) from the National Cancer Institute of NIH, Career Development Award from American Association of Cancer Research/Pancreatic Cancer Action Network (K.N. Sugahara), and Blasker Science Award from the San Diego Foundation (K.N. Sugahara). G.B. Braun was supported by CA121949 NIH T32 Fellowship, and T. Teesalu was supported by KG110704 Susan Komen for Cure Foundation Career Development Award, European Research Council Starting Grant (GliomaDDS), and Wellcome Trust International Fellowship (WT095077MA).

List of Abbreviations

VEGF	vascular endothelial growth factor
NRP-1	neuropilin-1
NRP-2	neuropilin-2
CendR	C-end Rule
iRGD	a cyclic peptide with an amino acid sequence of CRGDK/RGPD/EC (the CRGDKGPDC form was used in the current study)
CRGDK/R	a linear penta-peptide
PDAC	pancreatic ductal adenocarcinoma
KPC mice	mice with *Kras*$^{G12D/+}$
LSL-Trp53$^{R172H/+}$	Pdx-1-Cre mutations
DMEM	Dulbecco's Modified Eagle Medium
FBS	fetal bovine serum
BSA	bovine serum albumin
iNGR	a cyclic peptide with an amino acid sequence of CRNGRGPDC
PFA	paraformaldehyde
AgNPs	silver nanoparticles
NA	NeutrAvidin
PEG	polyethylene glycol
OPSS	orthopyridyl disulfide
MTT	3-(4,5-dimethylthiazol-2-yl)-2,5-diphenyltetrazolium bromide
ANOVA	analysis of variance
RGDfV	a cyclic peptide
iRGDD	a scrambled iRGD peptide with an amino acid sequence of CRGDDGPKC
CRGDC	a cyclic peptide
iRGD-AgNPs	iRGD-coated AgNPs
CRGDC-AgNPs	CRGDC-coated AgNPs

Sema3A	semaphorin 3A
Sema3F	semaphorin 3F
RPARPAR	a prototypic linear CendR peptide
RPARPAR-NH2	RPARPAR peptide with a blocked C terminus
CRGEC	a control peptide for CRGDC

References

1. McDonald DM, Baluk P. Significance of blood vessel leakiness in cancer. Cancer Res. 2002; 62:5381–5. [PubMed: 12235011]
2. Heldin CH, Rubin K, Pietras K, Östman A. High interstitial fluid pressure – An obstacle in cancer therapy. Nat Rev Cancer. 2004; 4:806–3. [PubMed: 15510161]
3. Prabhakar U, Maeda H, Jain RK, Sevick-Muraca EM, Zamboni W, Farokhzad OC, et al. Challenges and key considerations of the enhanced permeability and retention effect for nanomedicine drug delivery in oncology. Cancer Res. 2013; 73:2412–7. [PubMed: 23423979]
4. Fukumura D, Kashiwagi S, Jain RK. The role of nitric oxide in tumour progression. Nat Rev Cancer. 2006; 6:521–34. [PubMed: 16794635]
5. Zhou W, Fong MY, Min Y, Somlo G, Liu L, Palomares MR, et al. Cancer-secreted miR105 destroys endothelial barriers to promote metastasis. Cancer Cell. 2014; 25:501–15. [PubMed: 24735924]
6. Prud'homme GJ, Glinka Y. Neuropilins are multifunctional coreceptors involved in tumor initiation, growth, metastasis and immunity. Oncotarget. 2012; 3:921–39. [PubMed: 22948112]
7. Teesalu T, Sugahara KN, Ruoslahti E. Tumor-penetrating peptides. Front Oncol. 2013; 3:216. [PubMed: 23986882]
8. Teesalu T, Sugahara KN, Kotamraju VR, Ruoslahti E. C-end Rule: Peptides with C-terminal arginine cause neuropilin-1 dependent internalization, vascular leakage and tissue penetration. Proc Natl Acad Sci U S A. 2009; 106:16157–62. [PubMed: 19805273]
9. Sugahara KN, Teesalu T, Karmali PP, Kotamraju VR, Agemy L, Girard OM, et al. Tissue-penetrating delivery of compounds and nanoparticles into tumors. Cancer Cell. 2009; 16:510–20. [PubMed: 19962669]
10. Desgrosellier JS, Cheresh DA. Integrins in cancer: biological implications and therapeutic opportunities. Nat Rev Cancer. 2010; 10:9–22. [PubMed: 20029421]
11. Sugahara KN, Teesalu T, Karmali PP, Kotamraju VR, Agemy L, Greenwald DR, et al. Coadministration of a tumor-penetrating peptide enhances the efficacy of cancer drugs. Science. 2010; 328:1031–5. [PubMed: 20378772]
12. Feron O. Tumor-penetrating peptides: A shift from magic bullets to magic guns. Sci Transl Med. 2010; 2:34ps26.
13. Yang M, Jiang P, Sun FX, Hasegawa S, Baranov E, Chishima T, et al. A fluorescent orthotopic bone metastasis model of human prostate cancer. Cancer Res. 1999; 59:781–6. [PubMed: 10029062]
14. Tseng WW, Winer D, Kenkel JA, Choi O, Shain AH, Pollack JR, et al. Development of an orthotopic model of invasive pancreatic cancer in an immunocompetent murine host. Clin Cancer Res. 2010; 16:3684–95. [PubMed: 20534740]
15. Sugahara KN, Murai T, Nishinakamura H, Kawashima H, Saya H, Miyasaka M. Hyaluronan oligosaccharides induce CD44 cleavage and promote cell migration in CD44-expressing tumor cells. J Biol Chem. 2004; 279:4541–50. [PubMed: 14623895]
16. Braun GB, Friman T, Pang HB, Pallaoro A, de Mendoza TH, Willmore AMA, et al. Etchable plasmonic nanoparticle probes for cell biology. Nat Mater. 2014; 13:904–11. [PubMed: 24907927]

17. Ruoslahti E, Hayman EG, Pierschbacher MD, Engvall E. Fibronectin: purification, immunochemical properties, and biological activities. Methods Enzymol. 1982; 82:803–31. [PubMed: 7078457]
18. Olive KP, Tuveson DA. The use of targeted mouse models for preclinical testing of novel cancer therapeutics. Clin Cancer Res. 2006; 12:5277–87. [PubMed: 17000660]
19. Koivunen E, Gay DA, Ruoslahti E. Selection of peptides binding to the alpha 5 beta 1 integrin from phage display library. J Biol Chem. 1993; 268:20205–10. [PubMed: 7690752]
20. Alberici L, Roth L, Sugahara KN, Agemy L, Kotamraju VR, Teesalu T, et al. De novo design of a tumor-penetrating peptide. Cancer Res. 2013; 73:804–12. [PubMed: 23151901]
21. Saiki I, Murata J, Iida J, Sakurai T, Nishi N, Matsuno K, et al. Antimetastatic effects of synthetic polypeptides containing repeated structures of the cell adhesive Arg-Gly-Asp (RGD) and Tyr-Ile-Gly-Ser-Arg (YIGSR) sequences. Br J Cancer. 1989; 60:722–8. [PubMed: 2803948]
22. Murphy EA, Majeti BK, Barnes LA, Makale M, Weis SM, Lutu-Fuga K, et al. Nanoparticle-mediated drug delivery to tumor vasculature suppresses metastasis. Proc Natl Acad Sci U S A. 2009; 105:9343–8. [PubMed: 18607000]
23. Ye Y, Xu B, Nikiforovich GV, Bloch S, Achilefu S. Exploring new near-infrared fluorescent disulfide-based cyclic RGD peptide analogs for potential integrin-targeted optical imaging. Bioorg Med Chem Lett. 2011; 21:2116–20. [PubMed: 21349709]
24. Zanuy D, Kotla R, Nussinov R, Teesalu T, Sugahara KN, Alemán C, et al. Sequence dependence of C-end rule peptides in binding and activation of neuropilin-1 receptor. J Struct Biol. 2013; 182:78–86. [PubMed: 23462097]
25. Luo Y, Raible D, Raper JA. Collapsin: a protein in brain that induces the collapse and paralysis of neuronal growth cones. Cell. 1993; 75:217–27. [PubMed: 8402908]
26. He Z, Tessier-Lavigne M. Neuropilin is a receptor of the axonal chemorepellent Semaphorin III. Cell. 1997; 90:739–51. [PubMed: 9288753]
27. Parker MW, Linkugel AD, Vander Kooi AW. Effect of C-terminal sequence on competitive semaphorin binding to neuropilin-1. J Mol Biol. 2013; 425:4405–14. [PubMed: 23871893]
28. Neufeld G, Kessler O. The semaphorins: versatile regulators of tumour progression and tumour angiogenesis. Nat Rev Cancer. 2008; 8:632–45. [PubMed: 18580951]
29. Kruger RP, Aurandt J, Guan KL. Semaphorins command cells to move. Nat Rev Mol Cell Biol. 2005; 6:789–800. [PubMed: 16314868]
30. Bielenberg DR, Hida Y, Shimizu A, Kaipainen A, Kreuter M, Kim CC, et al. Semaphorin 3F, a chemorepulsant for endothelial cells, induces a poorly vascularized, encapsulated, nonmetastatic tumor phenotype. J Clin Invest. 2004; 114:1260–71. [PubMed: 15520858]
31. Serini G, Valdembri D, Zanivan S, Morterra G, Burkhardt C, Caccavari F, et al. Class 3 semaphorins control vascular morphogenesis by inhibiting integrin function. Nature. 2003; 424:391–7. [PubMed: 12879061]
32. Shin TH, Sung ES, Kim YJ, Kim KS, Kim SH, Kim SK, et al. Enhancement of tumor penetration of monoclonal antibody by fusion of a neuropilin-targeting peptide improves the antitumor efficacy. Mol Cancer Ther. 2014; 13:651–61. [PubMed: 24435448]
33. Woo S, Gomez TM. Rac1 and RhoA promote neurite outgrowth through formation and stabilization of growth cone point contacts. J Neurosci. 2006; 26:1418–28. [PubMed: 16452665]
34. Geiger B, Spatz JP, Bershadsky AD. Environmental sensing through focal adhesions. at Rev Mol Cell Biol. 2009; 10:21–33.
35. Prockop DJ, Kivirikko KI. Collagens: Molecular biology, diseases, and potentials for therapy. Annu Rev Biochem. 1995; 64:403–34. [PubMed: 7574488]
36. Valdembri D, Caswell PT, Anderson KI, Schwarz JP, König I, Astanina E, et al. Neuropilin-1/GIPC1 signaling regulates α5β1 integrin traffic and function in endothelial cells. PLoS Biol. 2009; 7:e1000025.
37. Bagri A, Tessier-Lavigne M, Watts RJ. Neuropilins in tumor biology. Clin Cancer Res. 2009; 15:1860–4. [PubMed: 19240167]
38. Nguyen DX, Bos PD, Massagué J. Metastasis: from dissemination to organ-specific colonization. Nat Rev Cancer. 2009; 9:274–84. [PubMed: 19308067]

39. Tumour-cell invasion and migration: diversity and escape mechanism. Nat Rev Cancer. 2003; 3:362–74. [PubMed: 12724734]

40. Luo Y, Raper JA. Inhibitory factors controlling growth cone motility and guidance. Curr Opin Neurobiol. 1994; 4:648–54. [PubMed: 7849520]

41. Maione F, Capano S, Regano D, Zentilin L, Giacca M, Casanovas O, et al. Semaphorin 3A overcomes cancer hypoxia and metastatic dissemination induced by antiangiogenic treatment in mice. J Clin Invest. 2012; 122:1832–48. [PubMed: 22484816]

42. Carmeliet P, Jain RK. Principles and mechanisms of vesel normalization for cancer and other angiogenic diseases. Nat Rev Drug Discov. 2011; 10:417–27. [PubMed: 21629292]

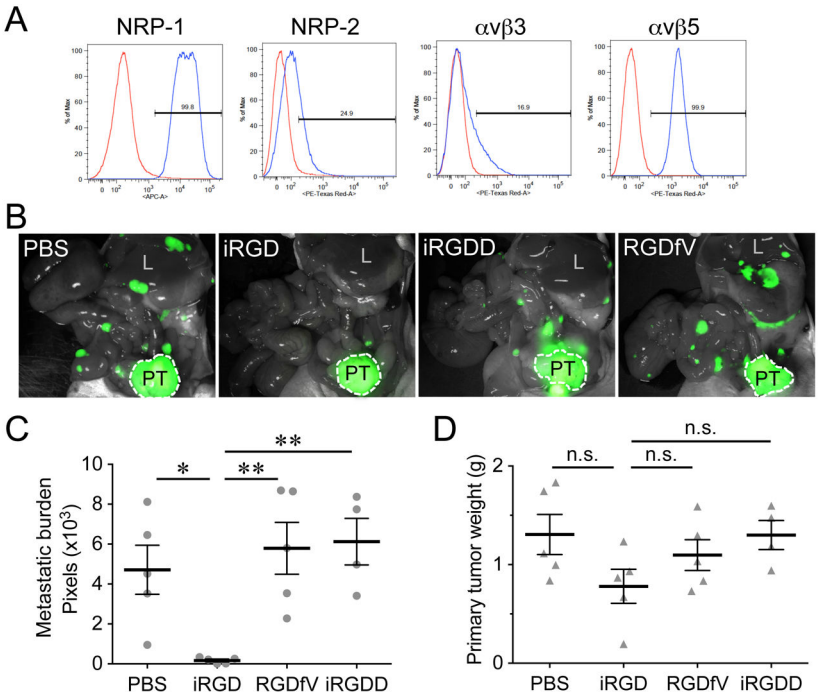

Figure 1. iRGD inhibts spontaneous metastasis in a prostate cancer mouse model

A, Neuropilin and αv integrin expression in GFP-PC-3 human prostate cancer cells analyzed by flow cytometry. The profiles represent the values of cells incubated with isotype control (red) or appropriate neuropilin (NRP) or integrin antibodies (blue) as primary antibodies. **B**, **C**, and **D**, Mice bearing orthotopic GFP-PC-3 tumors implanted 2 weeks earlier received intravenous injections of 4 μmol/kg of iRGD, a scrambled iRGD with a disrupted CendR motif (iRGDD: CRGDDGPKC), or a conventional non-CendR RGD peptide (RGDfV), or PBS, every other day for 21 days. The mice were necropsied after the treatment and viewed under a fluorescence imager (**B**). PT, primary tumor; L, liver. Metastatic burden was analyzed by quantifying fluorescence intensity with Image J (**C**). Weight of primary tumors (**D**). n = 5 per group. One of three experiments that gave similar results is shown. Error bars, mean ± SEM. Statistical analyses were performed with ANOVA: n.s., not significant; *P < 0.05; **P < 0.01.

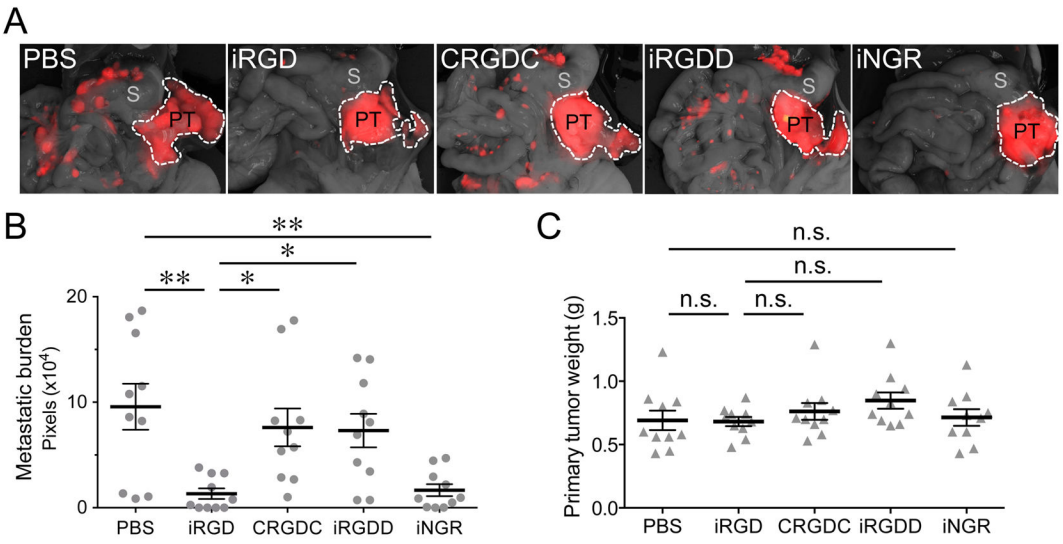

Figure 2. iRGD inhibits spontaneous metastasis in a pancreatic cancer mouse model

Mice bearing orthotopic LM-PmC mouse pancreatic tumors implanted 1 week earlier received intravenous injections of 4 μmol/kg of iRGD, a conventional non-CendR RGD peptide (CRGDC), iRGDD, or iNGR (CRNGRGPDC), or PBS, every other day for 14 days. n = 10 per group. One of two experiments that gave similar results is shown. **A**, The mice were necropsied after the treatment and viewed under a fluorescence imager. PT, primary tumor; S, stomach. **B**, Metastatic burden analyzed by quantification of fluorescence intensity with Image J. **C**, Weight of primary tumors. Error bars, mean ± SEM. Statistical analyses were performed with ANOVA: n.s., not significant; *P < 0.05; **P < 0.01.

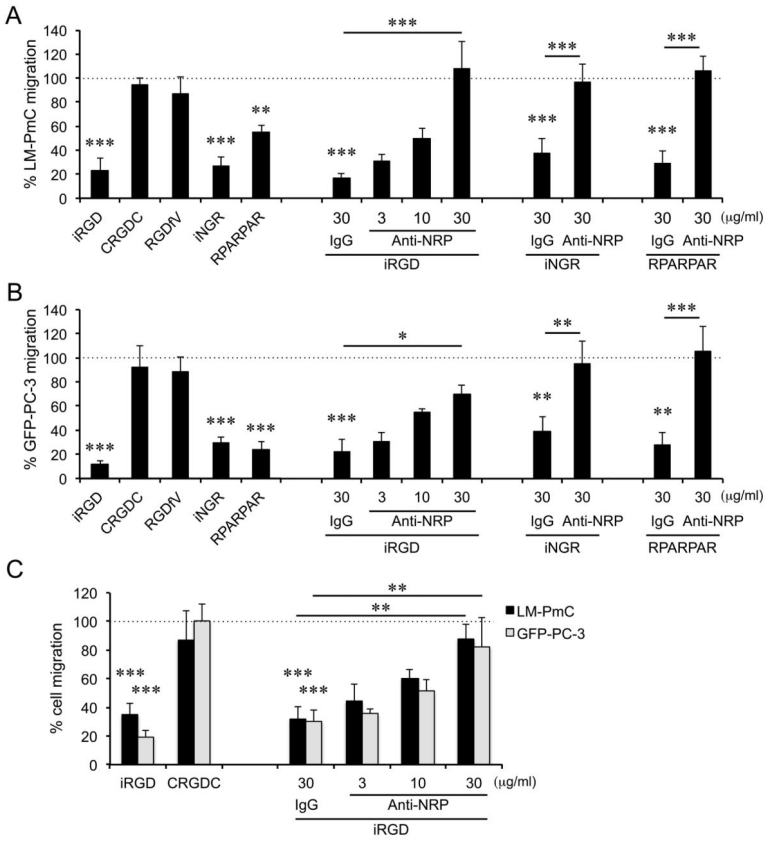

Figure 3. iRGD inhibits tumor cell migration in Transwell assays

LM-PmC (**A** and **C**) or GFP-PC-3 (**B** and **C**) cells were seeded on the upper side of a Transwell filter, and the number of cells that migrated to the other side of the filter was quantified. **A** and **B**, iRGD, non-CendR RGD peptides (CRGDC and RGDfV), or non-RGD CendR peptides (iNGR: CRNGRGPDC or RPARPAR) at a final concentration of 10 μM or PBS was added to both upper and lower wells. **C**, iRGD or CRGDC at a final concentration of 10 μM or PBS was added only to lower wells. Anti-NRP-1 b1b2 or control IgG was added to some of the wells. n = 3 per experiment. Non-treated columns were considered as 100%. Error bars, mean ± SEM; statistical analyses, ANOVA; *P < 0.05; **P < 0.01; ***P < 0.001. Statistics against the non-treated columns are shown unless otherwise noted.

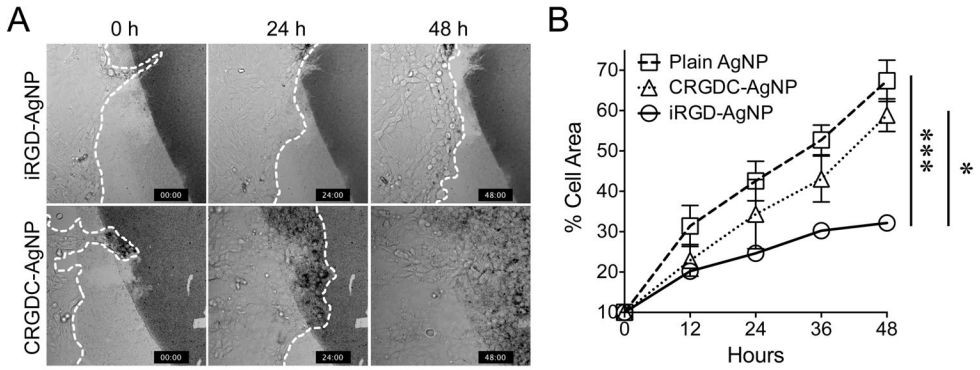

Figure 4. iRGD repels tumor cells

A, iRGD-coated silver nanoparticles (iRGD-AgNPs) or CRGDC-AgNPs were blotted on glass surfaces, and cells were seeded in the center in close proximity with the AgNPs. Cells were imaged for 48 hours. Representative images at 0, 24, and 48 hours are shown. The dark areas are coated with AgNPs. The dotted lines show the edge of the migrating cell populations. Note that the cells are repelled by iRGD-AgNPs, while they progressively migrate over CRGDC-AgNPs and completely saturate the field in 48 hours. n = 5. **B**, Cells were seeded on glass surfaces densely coated with the indicated AgNPs and imaged for 48 hours. The speed of cell migration was quantified by measuring %AgNP area covered by the cells. Error bars, mean ± SEM; statistical analyses, ANOVA; *P < 0.05; ***P < 0.001.

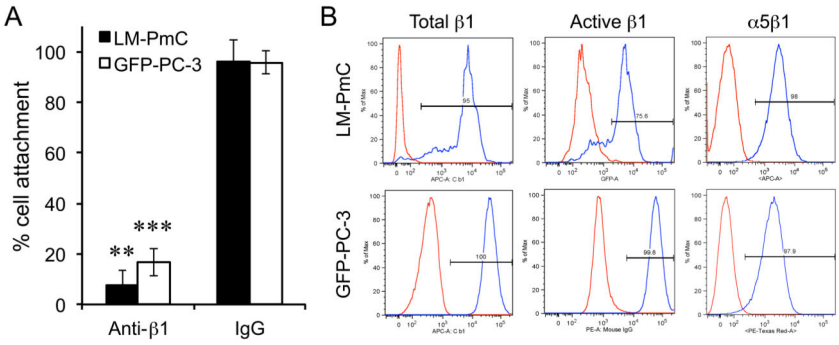

Figure 5. β1 integrin-dependent tumor cell attachment to fibronectin

A, LM-PmC (closed bars) or GFP-PC-3 (open bars) cells were seeded into 96-well plates coated with fibronectin, and allowed to attach for 30 minutes at 37°C in the presence of an anti-β1 integrin subunit antibody or a control IgG. The number of cells that remained attached to the wells were quantified. Cell attachment with no antibody was considered as 100%. n = 3. Error bars denote mean ± SEM. Statistical analyses were performed with Student's *t*-test: **P < 0.01; ***P < 0.001. **B,** Expression of total β1 integrins, β1 integrins in active conformation, and α5β1 integrin in LM-PmC and GFP-PC-3 cells analyzed by flow cytometry. The profiles represent the values of cells incubated with isotype control (red) or appropriate anti-β1, anti-active β1, or anti-α5β1 primary antibodies (blue).

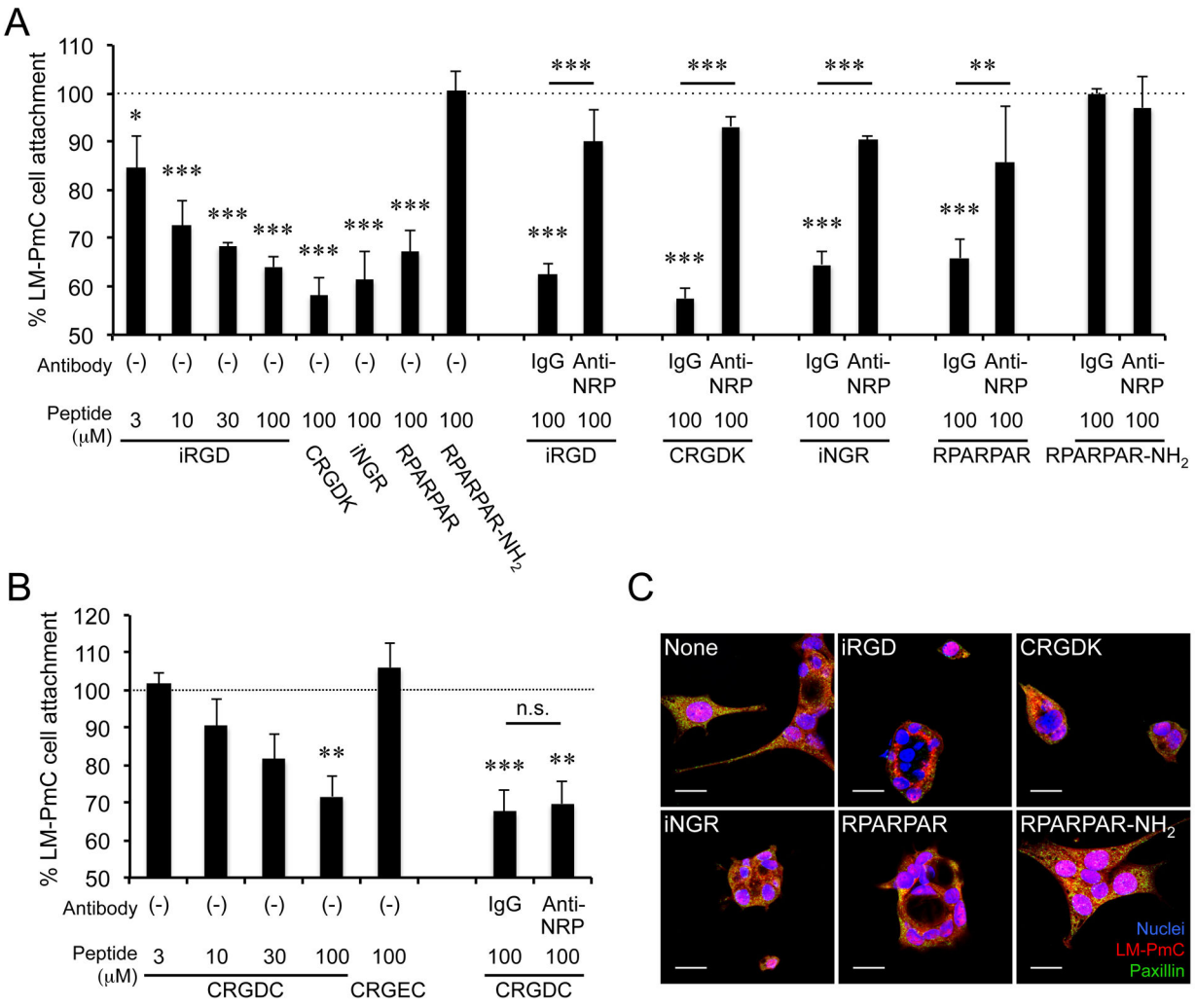

Figure 6. iRGD inhibits LM-PmC cell attachment to fibronectin in a NRP-1-dependent manner

A and **B**, Cell attachment assays. The number of LM-PmC cells that attached to fibronectin-coated wells in the presence of various peptides was quantified. In A, iRGD, cleaved iRGD with an inactive RGD motif (CRGDK), non-RGD CendR peptides (iNGR: CRNGRGPDC or RPARPAR), and a RPARPAR variant that lacks affinity to NRPs (RPARPAR-NH_2) were used. In B, a conventional non-CendR RGD peptide (CRGDC) and its non-integrin binding variant (CRGEC) were used. Some cells were also treated with anti-NRP-1 b1b2 or control IgG. n = 3 per experiment. Non-treated columns were considered as 100%. Error bars, mean ± SEM; statistical analyses, ANOVA; n.s., not significant; *P < 0.05; **P < 0.01; ***P < 0.001. Statistics against non-treated columns are shown unless otherwise noted. **C**, Cell retraction assays. LM-PmC cells (red) cultured on fibronectin-coated coverslips were treated with 10 μM of the indicated peptides for 1 hour, fixed, and stained for phospho-paxillin (green) and nuclei (blue). Representative confocal micrographs from three independent experiments are shown. Scale bars = 20 μm.